Spontaneous Oil-in-Water Emulsification Induced by Charge-Stabilized Dispersions of Various Inorganic Colloids

S. Sacanna,* W. K. Kegel, and A. P. Philipse*

Van't Hoff Laboratory for Physical and Colloid Chemistry, Debye Institute, Utrecht University, Padualaan 8, 3584 CH Utrecht, The Netherlands

Received May 7, 2007. In Final Form: July 24, 2007

Charge-stabilized dispersions of inorganic colloids are shown to induce spontaneous emulsification of hydrophobic (TPM) molecules to stable oil-in-water emulsions, with monodisperse, mesoscopic oil droplet diameters in the range of 30−150 nm, irrespective of the polydispersity of the starting dispersions. The results for cobalt ferrite particles and commercial silica sols extend our first study (Sacanna, S.; Kegel, W. K.; Philipse, A. *Phys. Rev. Lett.* **2007**, *98*, 158301) on spontaneous emulsification induced by charged magnetite colloids and show that this type of self-assembly is quite generic with respect to the composition of the nanoparticles adsorbing at the oil−water interface. Moreover, we provide additional experimental evidence for the thermodynamic stability of these mesoemulsions, including spontaneous oil dispersal imaged by confocal microscopy and monitored in situ by time-resolved dynamic light scattering. We discuss the possibility that thermodynamic stability of the emulsions is provided by the negative tension of the three-phase line between oil, water, and adsorbed colloids.

I. Introduction

A fundamental feature of coarse emulsions of oil in water is their thermodynamic instability, caused by the large amount of free energy "stored" in the droplets' interface. Such instability drives the system to minimize the interfacial area by coalescence of the oil droplets, which will eventually result in a complete separation of the constituent liquid phases. A well-known method of retarding such coarsening is the addition of finely divided solid particles that adsorb at the oil−water interface. This kind of emulsion stabilization, first described by Pickering[2]a century ago, is traditionally explained[3−5] as providing a mechanical barrier against coarsening and only recently[3] sparked a comparison of particles adsorbed at liquid−liquid interfaces to surfactants.

However, because mixtures of oil, water, and surfactant may form thermodynamically stable microemulsions,[6] this comparison harbors an intriguing scenario that is at odds with the kinetic explanation[3−5] of particle-stabilized emulsions, namely, the spontaneous distribution of oil in water to reproducible droplets stabilized by the action of colloidal particles. Recently,[1] we have demonstrated the existence of such a scenario for a methacrylate oil phase and charged magnetite nanoparticles that self-assemble in water to monodisperse (magnetizable) mesoscopic emulsion droplets. Direct evidence of this self-assembly was provided, among other things, by the spontaneous evolution of binary droplet mixtures toward one intermediate size distribution and by the existence of a maximum droplet radius with a concomitant expulsion of excess oil, by analogy to microemulsions.[1]

In this study, we also show that other charged inorganic colloids, namely, cobalt ferrite particles and commercial silica sols (Ludox), show this type of self-assembly, which apparently is quite generic and therefore potentially relevant for many other particle−oil systems. We also provide here new direct evidence of such self-assembly by monitoring the time evolution of polydisperse oil-in-water mixtures in contact with colloidal dispersions by confocal microscopy and time-resolved dynamic light scattering. Confocal microscopy shows macroscopic oil blobs that upon addition of colloids do not further coarsen but instead spontaneously deflate to much smaller magnetite-covered droplets. Similarly, time-resolved dynamic light scattering shows that polydisperse mixtures of oil, silica, and water above a critical particle/oil ratio self-assemble to silica-stabilized mesoemulsions with a narrow size distribution. Moreover, supporting transmission and scanning electron microscopy analyses, performed on polymerized emulsions, are used to characterize droplets morphologies and size distributions further.

Finally, we briefly discuss how the spontaneous emulsification of oil-in-water caused by the adsorption of nanoparticles at the oil−water interface could be driven by negative tension at the three-phase line between oil, water, and the inorganic colloids.

II. Experimental Section

A. Preparation. *Colloidal Dispersions.* Magnetite (Fe_3O_4) dispersions were prepared (see ref 7[7] for a detailed description) by adding aqueous acid solutions of $FeCl_2$ and $FeCl_3$ to ammonia, collecting the immediately precipitated black magnetite with a magnet, redispersing it overnight in a tetramethylammonium (TMA)−hydroxide solution (2 M), and transferring the magnetite particles to demineralized water via magnetic decantation. The final dispersion contained nonaggregated, negatively charged magnetite particles (average diameter 11 nm ± 28%). Aqueous dispersions of cobalt ferrite ($CoFe_2O_4$) particles (diameter 15 nm ± 21%) were obtained following[8] again repeptising to the black precipitate using TMA−hydroxide. Silica dispersions (Ludox, AS-40, DuPont) contained a weight concentration ($c = 50.8$ wt %) of unaggregated, amorphous silica particles (diameter 25 nm ± 18%) in an aqueous ammonium hydroxide solution and were used as received.

* Corresponding authors. E-mail: s.sacanna@chem.uu.nl; a.p.philipse@chem.uu.nl.

(1) Sacanna, S.; Kegel, W. K.; Philipse, A. *Phys. Rev. Lett.* **2007**, *98*, 158301.
(2) Pickering, S. *J. Chem. Soc.* **1907**, *91*, 2001−2021.
(3) Binks, B. P. *Curr. Opin. Colloid Interface Sci.* **2002**, *7*, 21−41.
(4) Walstra, P. Emulsions. In *Fundamentals of Interface and Colloid Science*; Lyklema, J., Ed.; Elsevier: Amsterdam, 2005; Vol. 5.
(5) Dickinson, E. *An Introduction to Food Colloids*; Oxford University Press: Oxford, U.K., 1992.
(6) Sottmann, T.; Strey, R. Microemulsions. In *Fundamentals of Interface and Colloid Science*; Lyklema, J., Ed.; Elsevier: Amsterdam, 2005; Vol. 5.
(7) Massart, R. *IEEE Trans. Magn.* **1981**, Mag-17.
(8) Tourinho, F. A.; Franck, R.; Massart, R. *J. Mater. Sci.* **1990**, *25*, 3249−3254.

10.1021/la701311b CCC: $37.00
Published on Web 09/07/2007

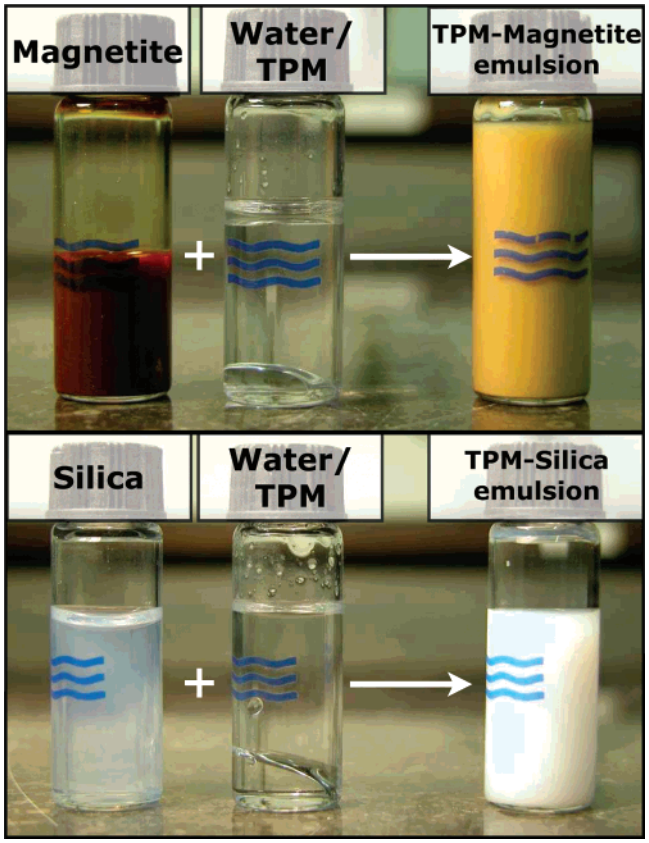

Figure 1. Mixing an aqueous dispersion of magnetite or silica nanoparticles into a phase-separated water−TPM mixture (TPM−oil is on the bottom) spontaneously produces an opaque oil-in-water emulsion stabilized by the adsorbed particles.

Emulsions. In a typical emulsification, a 100 mL dispersion of magnetite particles (c = 1.2 g/L) was gently agitated with 200 μL of methacryloxypropyltrimethoxysilane (TPM, Acros Organic p.a., used as received from new bottles), leading to stable emulsions as shown in Figure 1. Agitation is not a prerequisite: carefully pouring an aqueous magnetite dispersion layer onto TPM so as to leave the immiscible layers undisturbed also eventually yields (after a few days) stable emulsions. The particle-stabilized TPM droplets can be polymerized, as initiated by 0.4 mM potassium persulphate (KPS) at 80 °C or, when illuminated by UV light, at room temperature. Fluorescent emulsion droplets are obtained by incorporating into the oil phase the dye 4-methylaminoethylmethacrylate-7-nitrobenzo-2-oxa-1,3-diazol (NBD-MAEM) prepared according to ref 9.[9] This dye was also used to obtain the confocal microscopy images in Figure 6. Spontaneous TPM emulsification by cobalt ferrite particles occurred by the same procedure as for magnetite particles. Silica-stabilized emulsions were prepared by adding TPM to dilute Ludox dispersions. Typically, 1.5 mL of TPM and 1.5 mL of the Ludox dispersion were mixed with 40 mL of demineralized water. The final TPM/Ludox weight ratio was varied from 0.5 to 2.

B. Characterization. *Microscopy.* Confocal images were taken with a Nikon TE 2000U equipped with a Nikon C1 confocal scanning head, an Ar ion laser (Spectra Physics), and an oil immersion lens (100× CFI Plan Apochromat, NA 1.4 Nikon). Polymerized emulsion droplets were imaged by transmission electron microscopy (TEM, Philips TECNAI12) and scanning electron microscopy (SEM, Philips XLFEG30). TEM and SEM samples were prepared by drying drops of dilute dispersions on copper TEM grids and, when necessary (SEM), coating with a 7-nm-thick layer of a Pt/Pd alloy. Cryogenic electron microscopy (cryo-TEM) was used to image mesoemulsions in vitrified water films prepared by rapid temperature quenching in liquid ethane. For details, see ref 10[10] and references therein.

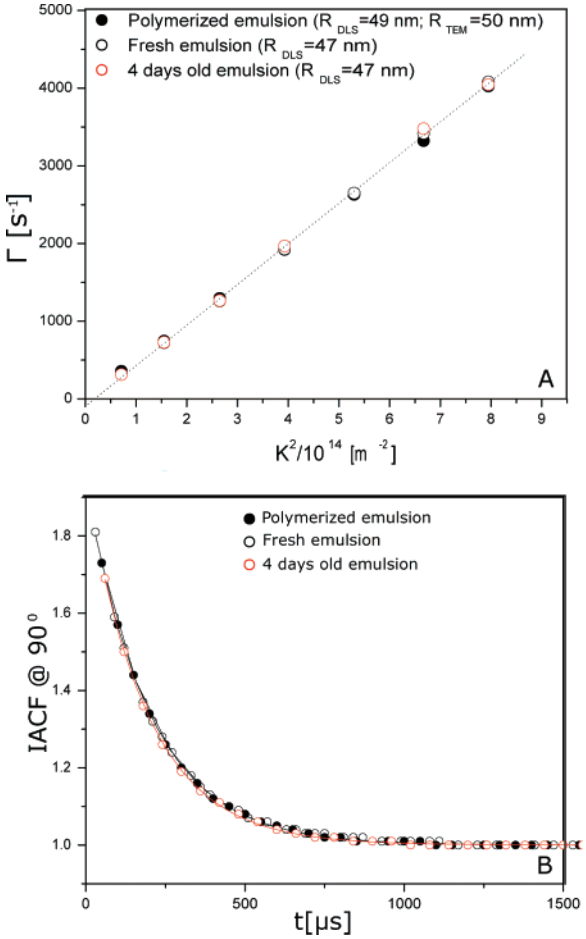

Figure 2. (A) Dynamic light scattering (DLS) data showing the decay rates of the scattered electric field autocorrelation functions (Γ) as a function of wavevector K^2 for a dilute magnetite-stabilized mesoemulsion, acquired before and after polymerization. As expected for monodisperse nonaggregated spheres, we obtained in both cases a linear plot with translational diffusion coefficients D_t (slope) corresponding to, respectively, R_{DLS} = 47 nm ($D_t = 5.23 \times 10^{-12}$ m^2 s^{-1}) and R_{DLS} = 49 nm ($D_t = 5.05 \times 10^{-12}$ m^2 s^{-1}). The average TEM radius for the polymerized emulsion droplets was 50 nm. (B) Typical DLS intensity autocorrelation functions (IACF) measured at 90° and their corresponding fitting lines.

Light Scattering. Dynamic light scattering (DLS) was performed on dilute emulsions at 25 °C using an argon ion laser (Spectra Physics) working at a wavelength of λ =514.5 nm and a power of 200 mW. Diffusion coefficients D_t were obtained by a cumulant fit of the measured scattering intensity autocorrelation functions.[11] The hydrodynamic droplets radii R_{DLS} were obtained by using the Stokes−Einstein equation

$$D_t = \frac{k_B T}{6\pi\eta R_{DLS}} \quad (1)$$

where k_B is the Boltzmann constant, T is the temperature, and η is the solvent viscosity.

Interfacial Tension. The surface tension γ of a TPM−water interface was determined at 25 °C using a spinning-drop tensiometer. The sample was prepared by first filling a Wilmad precision bore glass tube (i.d. 3.96 mm) with the dense phase (TPM), after which

(9) Bosma, G.; Pathmamanoharan, C.; de Hoog, E. H. A.; Kegel, W. K.; van Blaaderen, A.; Lekkerkerker, H. N. W. *J. Colloid Interface Sci.* **2002**, *245*, 292−300.

(10) Butter, K.; Bomans, P. H. H.; Frederik, P. M.; Vroege, G. J.; Philipse, A. P. *Nat. Mater.* **2003**, *2*, 88−91.

(11) Koenderink, G. H.; Sacanna, S.; Pathmamanoharan, C.; Rasa, M.; Philipse, A. P. *Langmuir* **2001**, *17*, 6086−6093.

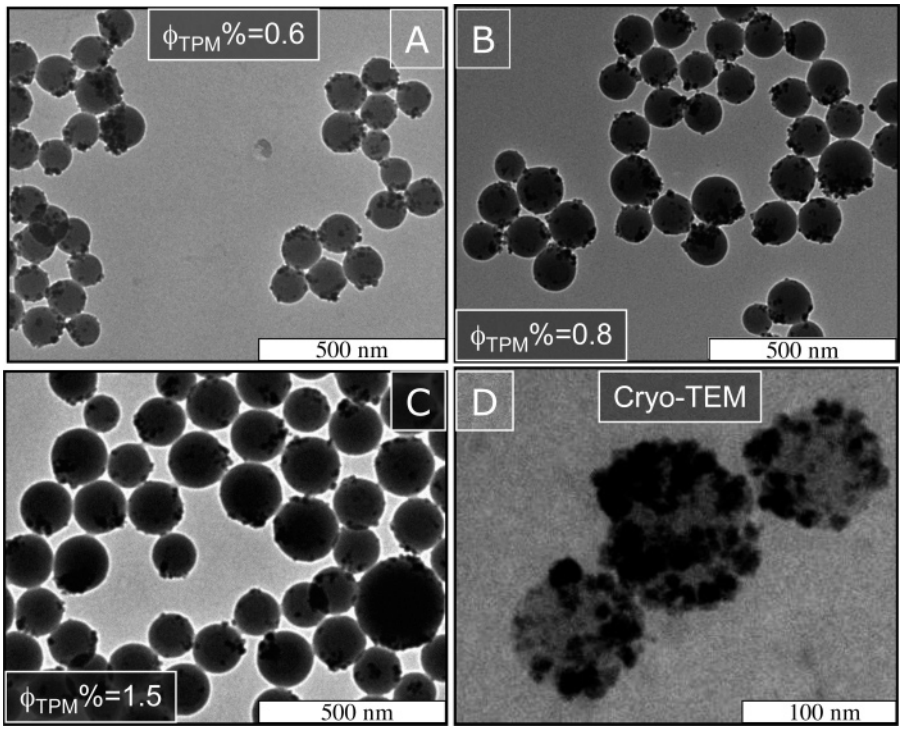

Figure 3. (A−C) Addition of TPM to water with a fixed magnetite concentration reproducibly increases the droplet radius, whereas addition of magnetite to a given amount of TPM decreases the radius. (D) High-magnification cryo-TEM images show emulsion droplets with a fairly dense magnetite coverage. This is not always the case for polymerized droplets where the nanoparticles seem to have clustered during the polymerization process.

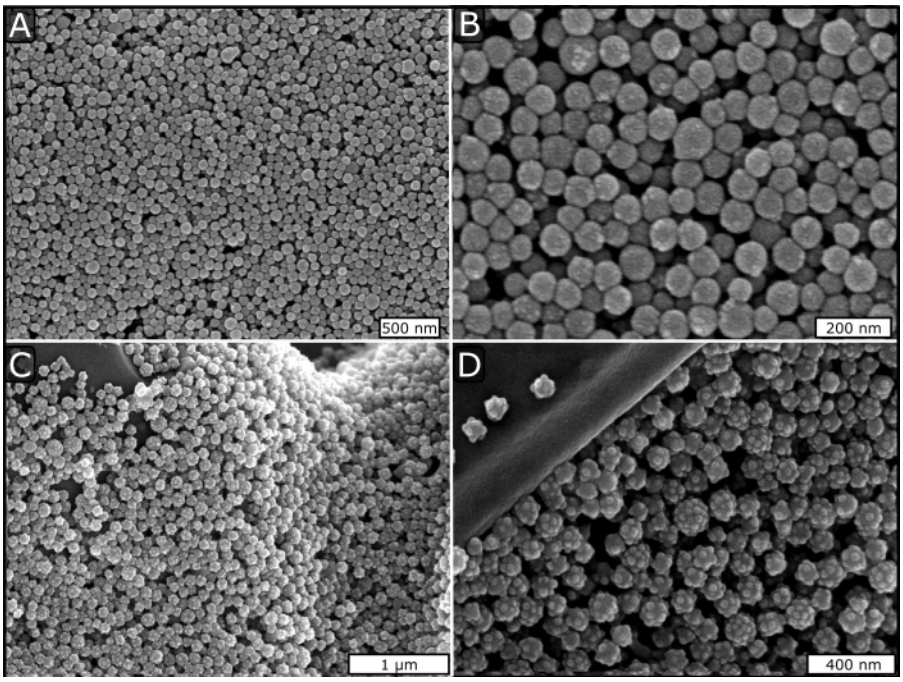

Figure 4. Scanning electron micrograph showing polymerized TPM emulsion droplets with adsorbed (A, B) magnetite and (C, D) silica Ludox particles visible as white spots on the droplet surfaces. Without polymerization, it is not possible to image an emulsion in this way.

a small drop of the less-dense phase (water) was injected. The angular velocity ω of the spinning tube was measured using an optical sensor, and the droplet was observed through a microscope. By measuring the droplet deformation due to the centrifugal field as a function of the rotational speed, the surface tension was determined using the Vonnegut equation[12,13]

$$\gamma = \frac{\Delta\rho\omega^2 r^3}{4} \qquad l > 4r \tag{2}$$

were $\Delta\rho$ is the density difference between the heavy and light phases (here $\Delta\rho = 4.5 \times 10^{-2}$ g cm^{-3}), r is the droplet radius perpendicular to the axis of rotation, and l is the droplet length along the axis of rotation.

(12) Vonnegut, B. *Rev. Sci. Instrum.* **1942**, *13*, 6−9.
(13) Princen, H. M.; Zia, I. Y. Z.; Mason, S. G. *J. Colloid Interface Sci.* **1967**, *23*, 99−107.

III. Results and Discussion

A. Spontaneous Emulsification. Figure 1 shows two examples of how magnetic nanoparticles (here magnetite)[1] and also small silica colloids can induce the spontaneous evolution of phase-separated TPM−water mixtures toward stable mesoemulsions. A gently agitated mixture of such components gradually increases its turbidity in a typical time span of 24 h, after which the opaque emulsion remains stably dispersed for days before any appreciable gravitational settling can be observed. The "shelf-life" behavior of such mesoemulsions manifests a narrow equilibrium size distribution. For sufficiently large average droplet size, emulsions slowly settle under gravity at a uniform (Stokes) velocity, producing an interface between the settling emulsion and the supernatant water phase that remains fairly sharp for several months. Droplet coalescence would have gradually blurred this interface in time because the Stokes velocity increases with the square of the droplet radius. Emulsion stability was further investigated by monitoring droplet size and polydispersity by dynamic light scattering (DLS). The narrow emulsion−droplet size distribution is confirmed by the DLS measurements of Figure 2: the decay rate of the scattered electric field autocorrelation function (Γ) increases linearly with wavevector K^2, as expected for monodisperse nonaggregated spheres.[11,14] Figure 2 also shows that DLS measurements performed on a freshly formed emulsion are virtually indistinguishable from measurements performed after aging the emulsion for 4 days. Coarsening would have eventually increased the average oil droplet size and polydispersity, causing the plot of Figure 2 to lower its slope and deviate from linearity.

The use of an acrylic oil phase, allowing the polymerization of emulsion droplets to solid particles, considerably facilitates system characterization by conventional TEM and SEM, which require dried samples. This circumvents the usual problems, such as the fixation of emulsions for electron microscopy,[6] in the analysis of droplets that are too small for imaging by light microscopy. Electron microscopy pictures, showing remarkably uniform particles (Figures 3 and 4), confirm that the oil phase in Figure 1 has dispersed to monodisperse mesoscopic droplets with the inorganic nanoparticles adsorbed at the oil−water interface.

The polymerization process does not change the droplet size, as demonstrated by the overlapping light scattering data shown in Figure 2 that were collected before and after the emulsion polymerization. However, cryo-TEM (Figure 3D) analyses on magnetite-stabilized mesoemulsions show droplets with a fairly dense coverage of particles, whereas conventional dry TEM pictures (Figure 3A−C) seem to display a smaller coverage. The latter is very likely because of the polymerization that apparently induces aggregation of magnetite particles on the droplet surface. Moreover, magnetite and cobalt ferrite particles, being quite polydisperse (up to 30%), have part of their size distribution close to the microscope resolution limit, which is therefore hardly distinguishable. Additional magnetic characterization of the magnetite- and cobalt ferrite-stabilized mesoemulsions together with an estimate of the magnetite coverage density can be found in ref 15.[15]

Analogous to magnetite and cobalt ferrite, the silica colloids in contact with TPM also self-assemble into mesoscopic oil droplets. Because of the larger size of the Ludox particles, SEM and TEM images offer more information about the oil droplet surface morphology, suggesting wetting angles close to 90°, and a somewhat higher particle coverage density than for the ferrite-stabilized emulsions (Figures 4C,D and 5B).

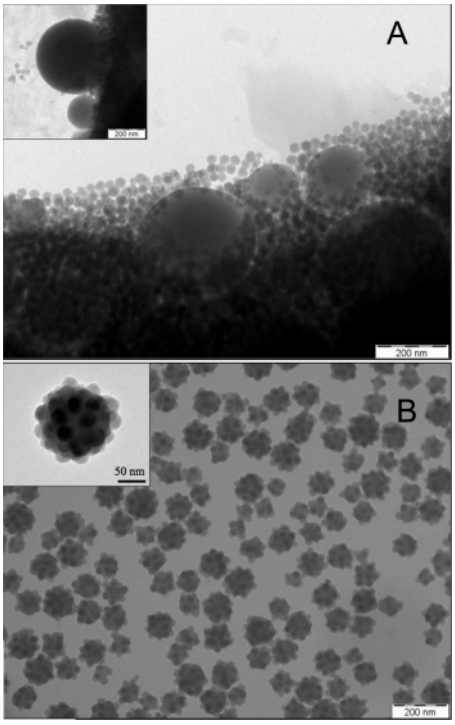

Figure 5. (A) Illustrative TEM images of unstable emulsions containing polydisperse blobs of phase-separated TPM surrounded by large quantities of small silica (Ludox) particles. (B) Above a critical TPM/Ludox weight ratio (Figure 8), oil and silica spontaneously emulsify to monodisperse Ludox-stabilized droplets, leaving no trace of free silica particles.

Another important observation is that TEM micrographs of stable mesoemulsions never display free nanoparticles. Apparently, the whole particle size distribution resides at the TPM−water interface, indicating a substantial adsorption free energy ΔG. Referring to the arguments in section IV, the latter can be estimated from the measured TPM−water interfacial tension ($\gamma = 8$ mN/m) to be on the order of $\pi R^2\gamma \approx 100kT$.

This essentially irreversible adsorption of nanoparticles does not prohibit reversible changes in droplet size because there is no barrier against the lateral diffusion of nanoparticles at the oil−water interface: they can accommodate the uptake or release of TPM molecules required to reach the equilibrium size distribution. The confocal images in Figure 6 show the importance of the (be it limited) solubility of TPM in water: the exchange of matter between droplets is sufficiently fast to reach the equilibrium curvature of the oil−water interface on a time scale of hours. Incidentally, the reduction of lateral mobility due to the agglomeration of nanoparticles is unlikely: the electrical-double-layer repulsion that separates these particles in the aqueous starting fluid will be enhanced by their adsorption onto an oil−water interface as a result of the low dielectric constant of the oil phase.[16] Besides oil, it should also be noted that surface material (i.e., colloids) should interchange for droplets to maintain their spherical shape. Whether this interchange involves individual nanoparticles or "patches" of surface (reminiscent of biological cell division) is yet unknown.

The most direct evidence for spontaneous oil dispersal in water, induced by nanocolloids (here, magnetite), is provided by confocal microscopy (Figure 6). In this experiment, a fixed 140 μm × 140 μm area positioned a few micrometers above the bottom glass

(14) Dhont, J. K. G. *An Introduction to Dynamics of Colloids*; Elsevier: Amsterdam, 1996.

(15) Sacanna, S.; Philipse, A. *Langmuir* **2006**, *22*, 10209−10216.

(16) Goulding, D.; Hansen, J. P. *Mol. Phys.* **1998**, *95*, 649−655.

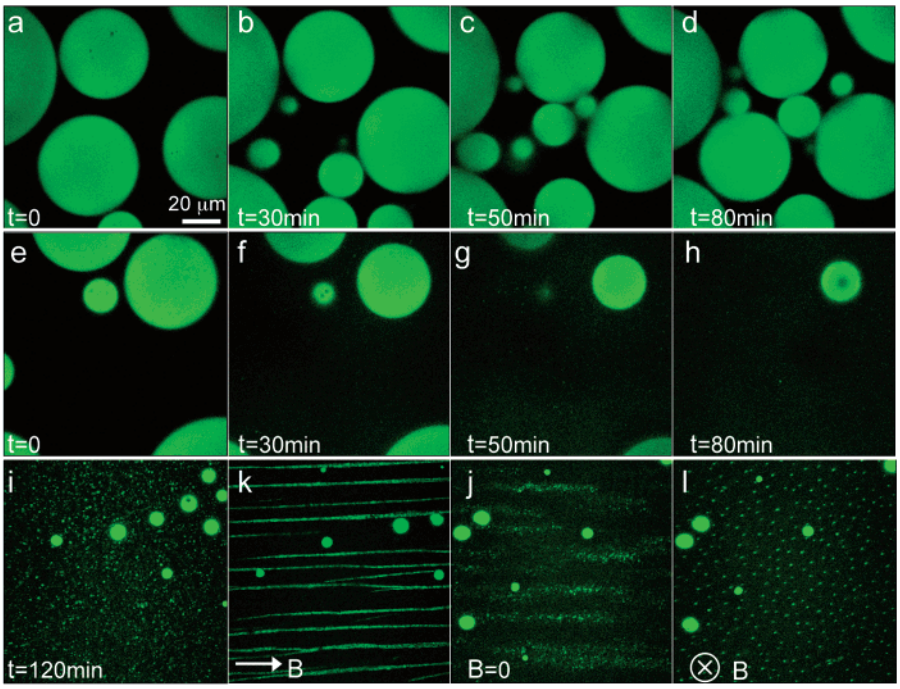

Figure 6. Snapshots from a confocal microscopy video (Supporting Information) showing (a−d) the coarsening of polydisperse TPM blobs in pure water and (e−h) the spontaneous deflation of these blobs once magnetite fluid has been added. After 2 h, (i) the TPM has been transferred to stable droplets covered with magnetite particles, as evidenced (k−l) by chain formation in a homogeneous magnetic field *B*. (k, j) The field is in the plane of the paper, and (l) the field was perpendicular to it such that a cross section of chains is observed. Chain formation is reversible, and (j) as soon as the field is switched off, the droplets diffuse freely again.

wall of the sample vial was imaged in time (3 h at 1/20 frames/s). In the absence of magnetite particles, we observe the coalescence of TPM in quiescent water to a macroemulsion of large polydisperse spheres. However, upon addition of magnetite fluid the coarsening stops and is actually reversed: we see that TPM blobs gradually shrink and disappear because oil disperses to uniform mesodroplets. The presence of adsorbed magnetite on the droplet surface is evident from the reversible chain formation in an external field (Figure 6k−l).

Evidence for spontaneous emulsification, in addition to its visual (Figure 1) and microscopic (Figure 6) manifestation, is also offered by time-resolved dynamic light scattering; as shown in Figure 7A, the evolution of a highly polydisperse system (mixture of TPM, water, and silica particles) to a monodisperse emulsion is characterized by only one diffusion coefficient. In this experiment, we performed DLS measurements at six different angles as a function of time from 30 min up to 48 h after preparing a sample with a TPM/silica weight ratio of 1.85. The plot of Figure 7A shows that the measured droplets radius R_{DLS} flattens in time to a nearly angle-independent value of 50 nm. After 48 h, no further changes were observed in the light scattering data, which indicates that the emulsification is complete and the oil droplets have reached their equilibrium size. DLS results are clearly supported by TEM and SEM images showing that emulsions polymerized after 48 h consist of monodisperse droplets (Figures 4C,D and 5B).

B. Droplet Size Control. One of the most striking features of our TPM mesoemulsions is their uniform, reproducible droplet size, despite the sometimes large polydispersity of the starting colloidal dispersions. For the magnetite-stabilized emulsions reported in ref 1,[1] we observed, at a given particle concentration, an initial linear dependence of the TPM droplet radius R_o on the TPM volume fraction, followed by a constant (maximum) value of R_o and the concomitant appearance of an excess oil phase in coexistence with the emulsion. This phase equilibrium, analogous to Winsor I in microemulsions,[17] is also observed here for the larger Ludox silica spheres, although in this case the droplet size control and emulsion stability window seem to be considerably reduced. Below a TPM/Ludox ratio of about 1.3, in fact, only unstable emulsions were formed (Figure 8), featuring macroscopic TPM droplets that rapidly settle by gravity and leave a large part of the small silica particles freely dispersed in the supernatant (water phase). Above this critical oil ratio, however, an abrupt transition occurs in which oil and silica self-assemble to stable mesoscopic emulsion droplets, causing the sample turbidity to increase significantly. The resulting milky emulsions remain stably dispersed for weeks before gravitational settling takes place. This transition is visually illustrated in Figure 8, which shows five samples at constant Ludox concentration ($c = 27.1$ g/L) and increasing oil volume fraction ϕ_o illuminated by a laser beam. For $\phi_o < 3.5\%$ (samples 1−3), the scattered beam is clearly visible because the samples mainly consist of silica nanoparticles in suspension with large unstable oil droplets that rapidly sediment and coalesce at the bottom of the vial. However, when ϕ_o rises above 3.5% (samples 4 and 5) the increased turbidity caused by the formation of stable mesoscopic droplets prevents the laser beam from crossing the samples. Visual observations are corroborated by electron microscopy analysis of polymerized samples. Indeed, samples in the unstable region (Figure 8, samples 1−3) show mixtures of highly polydisperse oil blobs in a "sea" of free silica particles (Figure 5A), whereas stable samples (Figure 8, samples 4 and 5) contain monodisperse emulsion droplets densely loaded with silica particle interfaces and show no evidence of free nanoparticles (Figures 5B), similar to the situation for magnetite- and cobalt ferrite-stabilized mesoemulsion droplets.

In the TPM−Ludox systems, no significant differences in droplet size could be achieved by varying the oil concentration. Instead, all of the stable emulsions comprise droplets having an average size of about 50 nm and a typical polydispersity of 16%.

(17) Winsor, P. A. *Trans. Faraday Soc.* **1948**, *44*, 376.

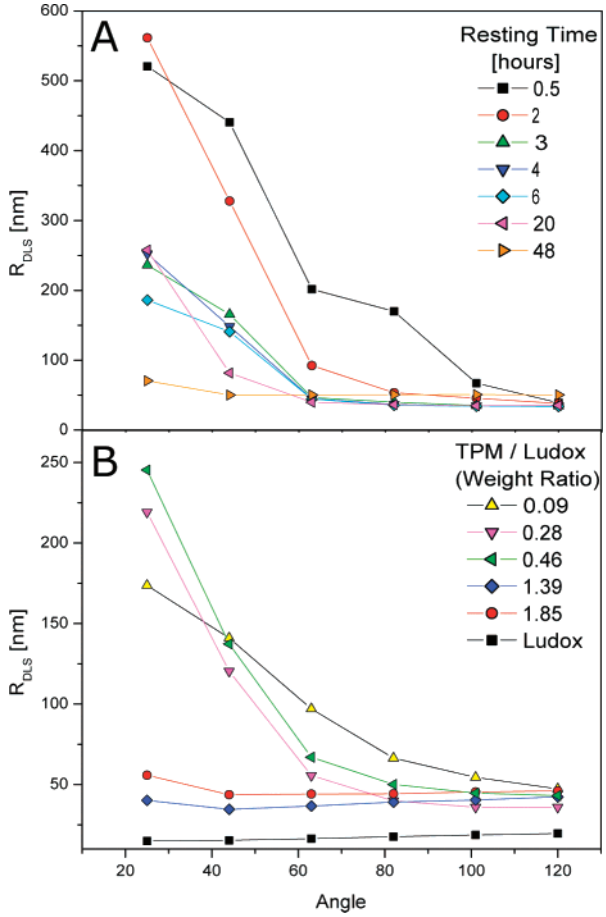

Figure 7. (A) Time-resolved DLS data demonstrating the evolution toward a stable emulsion with an angle-independent equilibrium size within 2 days after mixing the oil and silica dispersion above the critical weight ratio. The experiment was performed on a sample with a TPM/silica weight ratio of 1.85. (B) Emulsion droplet sizes from diffusion coefficients measured by DLS at different scattering angles. Note that for the aqueous dispersion of silica (Ludox) particles only, the obtained radius is angle-independent, as it should be for nonaggregated monodisperse particles. In the unstable region (TPM/silica weight ratio below 1.4), DLS clearly manifests light scattering by a highly polydisperse mixture, whereas above this ratio, the diffusion of monodisperse droplets is observed. Before the measurements, the emulsions in B were allowed to equilibrate for 24 h.

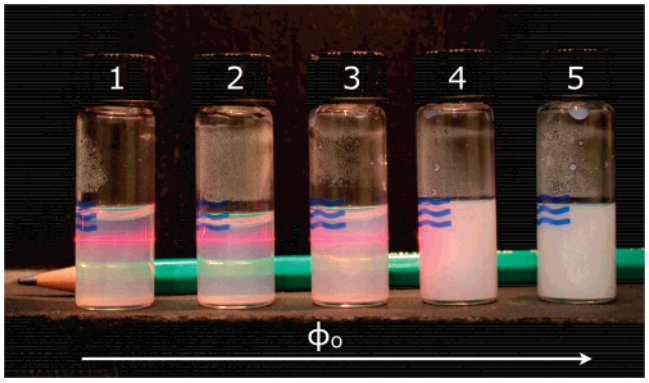

Figure 8. Typical example of the abrupt transition from unstable to stable TPM emulsions in water induced by colloidal silica (Ludox). Shown are samples with fixed Ludox concentration and increasing TPM concentration from left to right. Below a TPM/Ludox weight ratio of 1.4 (samples 1−3), emulsions are unstable, leading to the rapid sedimentation of silica aggregates and phase-separated TPM. (See also the TEM picture in Figure 5a.) Light scattering and TEM analyses show that a large number of free Ludox particles remain in the supernatant; they also scatter the light from a red laser passing through the samples. When the TPM/Ludox weight ratio exceeds 1.4 (samples 4 and 5), a sharp transition occurs for stable TPM−Ludox emulsions. TEM (Figure 5b) and DLS analyses demonstrate that all silica has self-assembled into monodisperse Ludox-stabilized emulsion droplets. The turbid emulsions remain homogeneous because the droplets are too small to settle under gravity.

IV. What Determines Thermodynamic Stability?

To address the question as to what determines the thermodynamic stability of our Pickering emulsions, we start from an aqueous dispersion of N colloids coexisting with an excess oil phase. This constrained state has a free energy equal to F_I. Note that we could also start with colloids in oil coexisting with excess water; this will not influence the final results of our analysis. Next we create a Pickering emulsion with an extensive colloid-loaded oil−water interface with a free energy of F_{II}. The interfacial work to create the Pickering emulsion is, per unit area per colloid,

$$\Delta f = \frac{F_{II} - F_I}{2\pi R^2 N} = \Delta\gamma(1 - z) + \frac{\gamma_L}{R}\sqrt{(1 - z^2)} + \frac{\gamma_{o/w}}{2}(\sigma - (1 - z^2)) \quad (3)$$

In this equation, R is the radius of a colloidal particle, and $\Delta\gamma = \gamma_{c/o} - \gamma_{c/w}$, with $\gamma_{c/w}$ and $\gamma_{c/o}$ being the interfacial tensions between colloid−water and colloid−oil. $\gamma_{o/w}$ is the oil−water interfacial tension, and γ_L is the (line) tension of the colloid−oil−water contact region. Furthermore, $zR = R\cos\theta$ is the distance between the plane of adsorption and the sphere center, where we count $z > 0$ if most of the particle surface sits in water and (thus) $z < 0$ if it sits in oil. σ is the average interfacial area (in units of πR^2) occupied by a colloidal particle. The first term in eq 3 combines the free-energy difference between particles at the interface and those fully immersed in water with the interactions between colloids and oil. The second contribution is due to the line tension of the adsorbed particles at the oil−water interface. The third term is the contribution of the "bare" oil−water interface: even if colloids are close packed in a hexagonal lattice, we have $\sigma = 2 - \sigma_{cp}$, with $\sigma_{cp} = \pi/2\sqrt{3}$ so that the bare oil−water interface will still make up roughly 10% of the total interface. Depending upon the value of the oil−water interfacial tension, this bare interface may embody a large positive contribution to the free energy. The second term in eq 3 is the only contribution to the free energy that may stabilize Pickering emulsions (i.e., it may lead to $\Delta f < 0$) because γ_L can in principle be smaller than zero. Clearly, for large R this contribution becomes negligible.

A negative sign of the line tension might be caused by the preferential adsorption of, for example, charged surfactants or amphiphilic salts at the region where oil, water, and colloid are in contact. (See, for example, refs 18 and 19.) In ref 20,[20] the influence of line tension on the adsorption of colloids at a pre-existing oil−water interface has been studied. As mentioned before, here we consider the conditions for the spontaneous extension of such an interface. A zeroth-order estimate of the magnitude of the line tension is

(18) Netz, R. R.; Andelman, D.; Orland, H. *J. Phys. II* **1996**, *6*, 1023−1047.
(19) Dan, N.; Safran, S. A. *Biophys. J.* **1998**, *75*, 1410−1414.
(20) Aveyard, R.; Clint, J. H.; Horozov, T. S. *Phys. Chem. Chem. Phys.* **2003**, *5*, 2398−2409.

$$|\gamma_L| \approx \frac{kT}{a} \quad (4)$$

with a being the molecular size (i.e., some average of the diameter of an oil and water molecule). This estimate leads to a line tension of several kT/nm. For comparable values of $\gamma_{c/w}$ and $\gamma_{o/w}$, the value of $\Delta\gamma$ will be in the range of $(10^{-3}-1)kT/nm^2$. Furthermore, a typical bare oil−water interfacial tension $\gamma_{o/w}$ is on the order of $10kT/nm^2$. However, even small amounts of an adsorbing species such as a partially hydrolyzed TPM may easily reduce that value by an order of magnitude. With these numbers, it is predicted that Pickering emulsions could be stabilized by colloids with radii up to 10−20 nm. Larger colloids are possible for smaller values of $\gamma_{o/w}$, but in general, the maximum radius is not expected to exceed a few tens of nanometers. Note that near first-order wetting transitions, line tensions of as low as $-50kT$/nm have been reported.[21,22] That would increase the maximum colloid size below which stable Pickering emulsions form even more.

Here we also note that for a better understanding of the emulsification mechanism it will be necessary to investigate the molecular details involved, including the oil chemical reactivity that might play an important role. In fact, beside the TPM radical polymerization, which occurs only in the presence of an initiator, we might conjecture a partial hydrolysis of the TPM silane alkoxide moiety that could yield surface-active anionic species such as $R-Si(OCH_3)_2O^-$ that are able to take part in the emulsification mechanism.[23] These issues are currently being studied.

V. Conlusions and Outlook

We have shown that the spontaneous self-assembly of nanoparticles and hydrophobic TPM molecules to stable mesoemulsions with uniform droplet size is not restricted to iron-containing particles.[1] Indeed, our observation that commercially available silica colloids also lead to thermodynamically stable Pickering emulsions implies that spontaneous emulsification is generic with respect to the nature of the nanoparticles.

Confocal microscopy and time-resolved dynamic light scattering demonstrate that the emulsification occurs via an inverse Ostwald ripening mechanism involving large oil droplets that spontaneously "deflate" to feed newly nucleating mesodroplets. The latter reach their final equilibrium size distribution typically within 24 h, after which no further changes occur. The mesodroplets have the potential to be reproducible carrier emulsions for various catalytic or other functional particles, besides being convenient seed dispersions for the preparation of magnetic core−shell latex particles[15] as well as a large variety of composite silica colloids.[24]

The thermodynamically stable nature of the mesoemulsions has been experimentally assessed. Negative line tension may drive spontaneous oil dispersal. However, the molecular details of the emulsification mechanism are still unclear. In particular, further research is required to clarify the role of the reactive oil phase with respect to the possible partial hydrolysis of the silane alkoxide moiety.

Acknowledgment. We thank H. Meeldijk (Electron Microscopy, Department of Biology, Utrecht) for assistance with the cryogenic electron microscopy. This work was financially supported by The Netherlands Organization for Scientific Research (NWO/Stichting Chemische Wetenschappen).

Supporting Information Available: Real-time confocal microscopy movie (140 μm × 140 μm image) showing magnetic, fluorescently labeled, stable mesoemulsion droplets that rapidly arrange into chains in a magnetic field that is alternatively applied in different directions. The droplets do not coalese, and chains dissolve by diffusion when the field is switched off. This material is available free of charge via the Internet at http://pubs.acs.org.

LA701311B

(21) Wang, J. Y.; Betelu, S.; Law, B. M. *Phys. Rev. Lett.* **1999**, *83*, 3677−3680.
(22) Pompe, T. *Phys. Rev. Lett.* **2002**, *89*, 076102/1−076102/4.
(23) Sacanna, S.; Rossi, L.; Philipse, A. *Langmuir*, accepted for publication, 2007.
(24) Sacanna, S.; Philipse, A. *Adv. Mater.* **2007**, in print.